

Chemical Modification of Cellulose for Biomolecule Capture

Arthur Yu

A thesis

submitted in partial fulfillment of the
requirements for the degree of

Master of Science in Bioengineering

University of Washington

2012

Committee:

Dr. Daniel M. Ratner

Dr. Barry R. Lutz

Program Authorized to Offer Degree:

Bioengineering

University of Washington

Abstract

Chemical Modification of Cellulose for Biomolecule Capture

Arthur Yu

Chair of the Supervisory Committee:

Professor Daniel M. Ratner

Department of Bioengineering

Paper-based analytical devices are the subject of growing interest for the development of low-cost point-of-care diagnostics, environmental monitoring technologies, and research tools for limited-resource settings. However, there are limited chemistries available for the conjugation of biomolecules to cellulose for use in biomedical applications. Herein divinyl sulfone (DVS) chemistry is demonstrated to covalently immobilize small molecules, proteins and DNA onto the hydroxyl groups of cellulose membranes through nucleophilic addition. Assays on modified cellulose using protein-carbohydrate and protein-glycoprotein interactions as well as oligonucleotide hybridization show that the membrane's bioactivity was specific, dose-dependent, and stable over a long period of time. Use of an inkjet printer to form patterns of biomolecules on DVS-activated cellulose illustrates the adaptability of the DVS functionalization technique to pattern sophisticated designs, with potential applications in cellulose-based lateral flow devices.

Table of Contents

| | |
|--|-----|
| List of Figures | iii |
| List of Tables | iv |
| Introduction* | 1 |
| Clinical Relevance | 1 |
| Precedent for Biomolecular Activation of Cellulose | 2 |
| Precedent for Use of Divinyl Dulfone | 3 |
| Objectives and Scope | 5 |
| Primary Objective | 5 |
| Secondary Objectives | 5 |
| Scope..... | 5 |
| Materials, Reagents and Methods* | 7 |
| Materials and Reagents..... | 7 |
| DVS Activation of Cellulose..... | 8 |
| Functionalization of DVS-activated Cellulose..... | 8 |
| Inkjet Functionalization of DVS+ Membranes..... | 9 |
| Surface Characterization of Modified Cellulose Membrane | 11 |
| Tensile Strength Characterization of Modified and Unmodified Cellulose..... | 12 |
| Lateral Flow Characterization of Modified and Unmodified Cellulose and Nitrocellulose..... | 12 |
| Preparation of Labeled Carbohydrate-Binding Protein Probes | 13 |
| Preparation of Labeled Nucleotide Probes..... | 13 |
| Colorimetric Detection of Immobilized Biomolecules..... | 14 |

| | |
|--|----|
| Fluorometric Detection of Immobilized Biomolecules | 15 |
| Analysis of Assayed Membrane | 16 |
| Results and Discussion | 18 |
| Cellulose Surface and Material Characterization | 18 |
| Lateral Flow Speed of Modified and Unmodified Cellulose and Nitrocellulose | 20 |
| Detection of Carbohydrate-Protein Interactions | 21 |
| Detection of FITC-Alginate..... | 25 |
| Detection of DNA Oligonucleotide Hybridization..... | 26 |
| Detection of Protein-Protein Interactions | 29 |
| Stability of DVS-activated Cellulose..... | 30 |
| Printed Biomolecular Patterning..... | 32 |
| Conclusions..... | 34 |
| References..... | 35 |
| Appendix..... | 40 |
| Appendix 1: Schematics of Biomolecules and DNA Hybridization Experiments | 40 |
| Appendix 2: Photographs of Bioprinter Modification | 42 |

List of Figures

| | |
|--|----|
| Figure 1: Project chemical theory and practical method summary..... | 6 |
| Figure 2: Epson inkjet printer modification for biomolecule functionalization..... | 10 |
| Figure 3: BioDot apparatus set up for assay..... | 14 |
| Figure 4: ImageJ ROI analysis for intensities..... | 17 |
| Figure 5: SEM micrographs of cellulose..... | 19 |
| Figure 6: LF speed through variety of paper types..... | 20 |
| Figure 7: Colorimetric-based detection of glycan-lectin interactions..... | 22 |
| Figure 8: Dose-dependent response of glycan-lectin interactions..... | 23 |
| Figure 9: Fluorometric-based detection of glycan-lectin interactions..... | 24 |
| Figure 10: Detection of alginate on DVS+ membranes..... | 26 |
| Figure 11: Fluorometric-based detection of DNA hybridization..... | 28 |
| Figure 12: Detection of anti-Streptavidin antibodies on DVS+ membranes..... | 30 |
| Figure 13: Stability of DVS+ chemistry | 31 |
| Figure 14: Stability of functionalized DVS+ membranes..... | 32 |
| Figure 15: Fluorescent visualization of inkjet-printed glycan patterns..... | 33 |
| Figure 16: Immobilized biomolecules used in this work..... | 40 |
| Figure 17: DNA functionalization and hybridization procedures..... | 41 |
| Figure 18: Photograph of bioprinter modifications..... | 42 |
| Figure 19: Photograph of bioprinter modifications 2..... | 43 |
| Figure 20: Photograph of bioprinter modifications 3..... | 43 |

List of Tables

| | |
|---|----|
| Table 1: Oligonucleotide sequences and modifications..... | 8 |
| Table 2: Relative Compositions of Functionalized Cellulose Determined by XPS..... | 18 |

Acknowledgements

The author thanks Dr. Daniel M. Ratner for his constant support and advice as my primary investigator and Department of Bioengineering faculty advisor, and Dorian Taylor for her guidance as graduate academic advisor.

The author thanks the members of the Ratner Lab for their support and valuable insight. In particular I would like to acknowledge Fang Cheng for his guidance on using the Bio-Dot apparatus, Jing Shang for her guidance on biological interactions discussed in this work, on Mr. James Kirk for data plot creations in this work, and Lauren Cummings for the SEM micrographs included in this work.

Introduction*

Some text has been adapted from the first author paper "Chemical Modification of Cellulose for Biomolecule Capture."

Clinical Relevance

Distributed diagnostics in the form of assays run on "lab-on-a-chip" platforms is a topic of great interest in global health because of their reach into low-resource settings. These typically low-cost platforms often employ lateral flow (LF) as an ideal solution for self-powered, rapid fluid flow within these devices.¹⁻³ For instance, nitrocellulose-based diagnostic strips employ LF for the transport of solutions over immobilized biomolecules (often antibodies) for analyte detection.⁴ Cellulose, a cheaper and non-hazardous alternative to nitrocellulose, has also recently attracted interest as a LF-based diagnostic platform for low-resource settings.⁵⁻⁸ Advantages of cellulose include low production costs, portability, durability, and excellent wicking ability of aqueous solutions via capillary action. Various cellulose-based diagnostic designs have been introduced, such as microfluidic paper analytical devices (μ PADs), 2D-shaped LF strips, and thread-based networks.⁸⁻¹¹ These designs vary in sophistication but typically feature isolated channels that wick aqueous solution to a test site; many operate multiple channels simultaneously to demonstrate multiplexing potential. For example, the simple branched design of the μ PAD allows a drop of reagent to be transported via capillary action to multiple test sites, yielding colorimetric readouts within minutes. The low-cost and timely convenience demonstrated by the μ PAD is a major advantage to operating diagnostics on cellulosic materials. However, further development of diagnostic devices on cellulose is limited by the need for a reliable strategy to immobilize bioactive molecules and impart selective and specific function to cellulose.

Precedent for Biomolecular Activation of Cellulose

Physical adsorption is the simplest strategy for biomolecule immobilization onto solid substrates. In particular, immobilization of proteins onto supports such as polyvinylidene difluoride (PVDF) and nitrocellulose is well documented.¹²⁻¹⁴ While proteins do interact with slightly anionic cellulose,¹⁵ physical adsorption is unlikely to be effective for biomolecules without cationic character, as they are less firmly bound and easily washed off. This is especially relevant when considering immobilization of small molecule ligands such as carbohydrates, as well as nucleic acids.

Recently, significant attention has been directed towards the chemical modification of cellulose for biomolecule functionalization. For example, carbonyldiimidazole and 1-cyano-4-dimethylaminopyridinium tetrafluoroborate were used by Stollner et al. to immobilize glucose oxidase and a glycosylated pentapeptide onto a cellulose dialysis membrane to form part of an immunosensor.¹⁶ The Nahar group has developed a UV-based activation strategy using 1-fluoro-2-nitro-4-azidobenzene to generate nitrenes from the azido group and subsequently immobilize unmodified carbohydrates and proteins to the cellulose.^{17,18} In a case of industrial interest, several methods for immobilizing invertase EPSON inkjet printer on Granocel cellulose carriers (e.g., NH₂-Granocel generated with pentaethylenhexamine, 1-chloro-2,3-epoxypropane sodium borohydride) have been explored to increase the enzyme's activity.⁹ Kong et al. presented an epichlorohydrin method for coupling DNA aptamers to cellulose beads to form an immunoadsorbent that could remove anti-DNA antibodies from the plasma of systemic lupus erythematosus patients.²⁰ Immobilized DNA has also been demonstrated to detect ATP by Su et al.; sodium periodate was used to generate aldehyde groups on cellulose that could then bind DNA aptamers.²¹ Most recently, Catarina et al. used the linking agent a 1,4-

phenylenediisothiocyanate, to immobilize DNA onto filter paper for target hybridization via capillary action,²² and Xu et al. detailed the fabrication of bioactive cellulose via heteropolysaccharide oxidation by galactose 6-oxidase²³.

Precedent for Use of Divinyl Sulfone

While the aforementioned covalent biomolecular immobilization strategies have successfully demonstrated the potential for chemical modification of cellulose, they are not without their limitations. Most methods require multiple modification steps, involve flammable and hazardous solvents, and are suitable only for specific classes of biomolecules. Therefore, a simple and versatile technique to immobilize a variety of biomolecules onto cellulose is highly desirable. To achieve this aim, use of divinyl sulfone (DVS) in a simple, two-step method for the covalent modification of cellulose with an assortment of biomolecules is reported. The homobifunctional DVS molecule contains two electrophilic vinyl groups which exhibit cross-linking activity with nucleophiles.²⁴ It has been reported to cross-link agarose to increase enzyme-adsorption, and to modify sepharose with mannose to form an adsorbent for a mannose-binding protein.^{25,26} In particular, Fornstedt et al. utilized DVS's cross-linking ability to generate D-mannose-substituted sepharose to capture and purify a *Vicia ervilia*-derived lectin.²⁶ Recently, our lab used DVS to functionalize hydroxyl-terminated gold surfaces and organophosphonate-coated silicon photonic microring resonators with glycans for biosensing applications.^{27,28} Cellulose, which contains many hydroxyl groups on its backbone, presents an ideal surface for functionalization. The chemical strategy involves addition of one of the vinyl groups to the cellulose backbone. Application of nucleophile-bearing biomolecules, either by spotting or inkjet printing, to the

remaining unreacted vinyl groups covalently attaches the biomolecules to the cellulose backbone.

Objectives and Scope

Primary Objective

The primary objective of the work in this thesis is the translation of DVS-based chemistry to cellulose for the immobilization of biomolecules. The biomolecular ligands of interest include glycans such as unmodified sugars and glycoprotein, DNA oligonucleotides and proteins. Ligands that are successfully immobilized onto cellulose should be detected by labeled biomolecules known to interact with those ligands, in fluorometric or colorimetric assay format.

Secondary Objectives

Secondary objectives for this work will be undertaken if the immobilization technique is successful in immobilization a variety of the aforementioned ligands. These will take the form of translations of the bioactive paper to other surface-based work such as bio-inkjet printing of biomolecules or integration into microfluidic-based valves. Another objective will be development of analyte detection in clinically relevant solutions such as human serum.

Scope

The scope of this project covers the chemical modification of cellulose, characterization of the morphology and chemical content of modified and unmodified cellulose, functionalization and subsequent verification of biofunctionalization of modified cellulose via label-based assays, and translation of an existing bio-printing technique onto modified cellulose. Most of these steps are documented graphically in Figure 1 below.

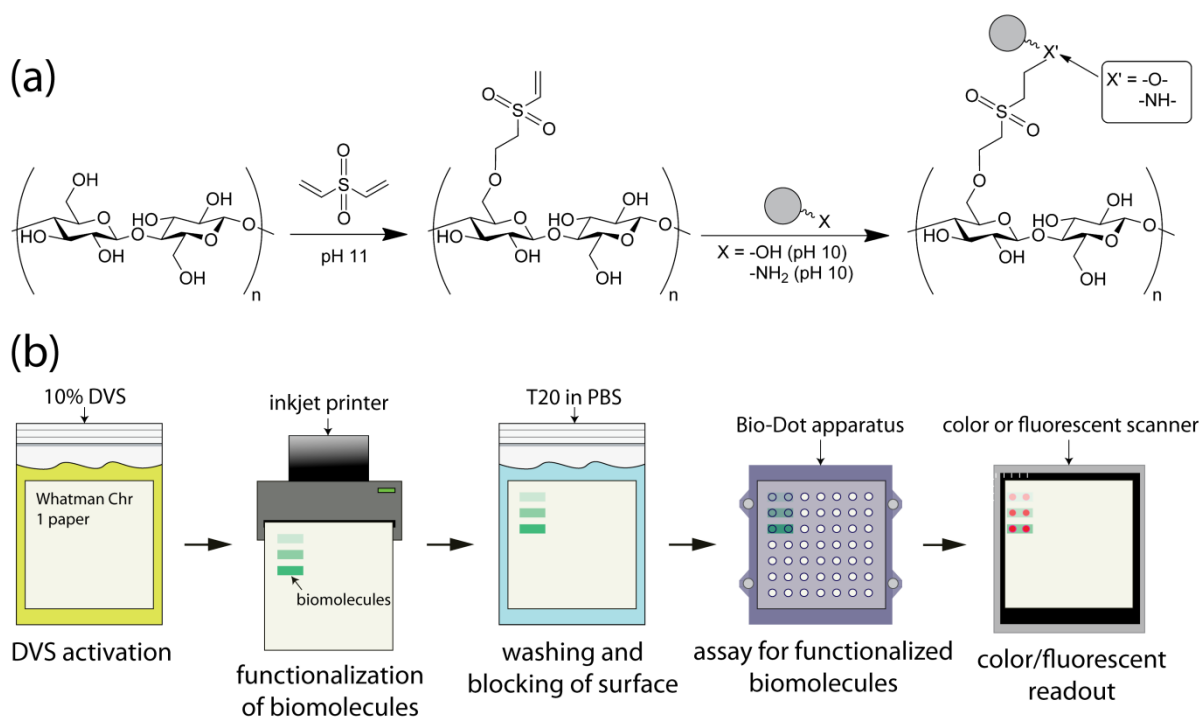


Figure 1. (a) Chemical activation and functionalization of cellulose with nucleophile-bearing biomolecules (gray). (b) Schematic of the stepwise process for paper activation via DVS, patterning of biomolecules via inkjet printing, and assaying of bioactivity.

Materials, Reagents and Methods*

Some text has been adapted from the first author paper "Chemical Modification of Cellulose for Biomolecule Capture."

Materials and Reagents

Chr 1 Chromatography paper (Whatman) was purchased from Sigma-Aldrich, St. Louis, MO. Nitrocellulose with capillary speed 135 sec/4cm was provided by Gina Fridley from the University of Washington. 97% DVS stabilized with 0.05% hydroquinone was purchased from Alfa Aesar, Ward Hill, MA. D-(+)-Mannose, D-(+)-Galactose, D-(+)-Maltose, D-(+)-Glucose and D-(+)-Lactose, Sucrose >98% pure powder and anti-Streptavidin antibody were purchased from Sigma-Aldrich, St. Louis, MO. Aminopropyl mannoside and aminopropyl galactose were synthesized as previously described.²⁹ Synthesis of the aminated Hexafluorobenzamide provided by Rodrigo B. Andrade and Justin Kaplan from Temple University is described in Appendix 1. Fluorescein Isothiocyanate-labeled alginate was provided by Gina Fridley. Horseradish peroxidase (HRP)-labeled Concanavalin A (Con A-HRP) and streptavidin was purchased from Sigma-Aldrich, St. Louis, MO. HRP-labeled Ricinus communis (RCA120-HRP) was purchased from EY Laboratories, San Mateo, CA. Dylight 649 amine-reactive dye was purchased from Thermo Fisher Scientific, Rockford, IL. RNase B was purchased from New England Biolabs, Ipswich, MA. PBS buffer (2.7 mM KCl, 137 mM NaCl, 10 mM phosphate, pH 7.4) and HEPES buffer (10 mM HEPES, 150 mM NaCl, 1 mM Ca²⁺ and Mn²⁺, pH 7.4) were prepared in the lab. Two complementary oligonucleotide sequences were purchased from Invitrogen Corporation, Carlsbad, CA. The sequences (A and A') are detailed in Table 1:

Table 1. Oligonucleotide Sequences and Modifications

| | 5' modification | Sequence | 3' modification |
|----|------------------|----------------------|-----------------|
| A | -NH ₂ | CTGAACGGTAGCATCTTGAC | None |
| A' | -NH ₂ | GTCAAGATGCTACCGTTCAG | None |

DVS Activation of Cellulose.

A 10% DVS (v/v, 0.1 M sodium carbonate, pH 11) solution was used to chemically activate cellulose membranes; 0.1 M sodium carbonate buffer alone served as a control (referred to in the text as DVS-). 12.0 x 9.0 cm sheets of Chr 1 paper were immersed in either 20 mL 10% DVS solution or in buffer alone, incubated in separate 400 mL-capacity plastic zip-bags, and agitated for 2 h on a rocking shaker. Following the incubation, the DVS-activated (DVS+) and control membranes (DVS-) were removed from the bags and rinsed in a plastic tray with 100 mL Millipore-purified deionized water, three times. These membranes were dried for 2 h in ambient conditions. In cases where the activated membranes were stored, they were either placed in aluminum foil in ambient conditions to protect from light and dust, or stored in a dry, nitrogen-filled plastic box.

Functionalization of DVS-activated Cellulose.

To test the potential for biofunctionalization of DVS-activated cellulose, DVS+ and DVS- membranes were manually spotted with nucleophile-bearing biomolecules. Free reducing sugars (at concentrations ranging from 292 to 1100 mM) and aminopropyl glycosides (at concentrations

ranging from 1 to 10 mM) were dissolved in 50 mM sodium carbonate buffer (pH 10). The glycoprotein RNase B was dissolved at 7 mM in PBS. The anti-Streptavidin antibody was dissolved at 25 μ M in PBS. FITC-alginate was dissolved at 3% of original dry mass in PBS (see "Detection of FITC-Alginate" in the Results and Discussion for detail on the motivation for immobilization alginate on DVS+ membranes). The oligonucleotide sequence A was dissolved at either 0.1 or 1 mM in PBS. 2 μ L volumes of these biomolecule solutions were spotted on the DVS+ and DVS- membranes in a 96-well grid format using a custom-made 96-well microplate template. On both membranes one row was not functionalized, to serve as a control for the non-specific binding of probes during detection assays. The spotted sheets were placed in a 75% relative humidity (RH) box at room temperature to react overnight. The sheets were then immersed in 20 mL PBS-T (0.05% w/v Tween® 20 in PBS) for 1 h in plastic zip-bags to block the surface and remove unbound biomolecules.

Inkjet Functionalization of DVS+ Membranes

In addition to manual spotting of biomolecules, automated techniques to spot biomolecules onto DVS+ membranes were separately explored. To pattern free galactose on the DVS+ membrane, an Epson R280 printer was modified using a method developed by James Wong and Barry Lutz from the Department of Bioengineering (mf20.org). This setup is depicted in Figure 2 below:



Figure 2. EPSON R280 inkjet modifications for printing carbohydrate bio-inks; uncovered printing mechanism including cartridges, inkjet, and DVS-activated sheet taped onto normal printer paper, ready to be printed with bio-ink.

Stock Epson ink cartridges were replaced with empty refill cartridges, and the ink channel of the black ink cartridge was hollowed out via a milling machine to allow a pipette tip to be fitted onto the printhead (in lieu of the cartridge's ink channel). Bioprinting solution was injected into the pipette tip; this served as the bioprinting solution reservoir. We devised a bioprinting solution composed of 10% w/v galactose, 40% w/v sucrose and 5% w/v TWEEN® 20 in 0.1 M pH 10 sodium carbonate buffer. Prior to printing the solution, 5 mL of a priming solution composed of

50% w/v sucrose and 5% w/v TWEEN® 20 in Millipore water was passed through the printhead via a syringe. This printing preparation process is more completely photographically documented in Appendix 2. The printed sheet was placed in the 75% RH box to react overnight and blocked, as previously described.

Surface Characterization of Modified Cellulose Membrane

To investigate changes in the content of the cellulose membranes as a result of activation and biomolecule functionalization, X-ray photoelectron spectroscopy (XPS) was employed. XPS composition data of the DVS+ and DVS- cellulose membranes were acquired on a Surface Science Instruments S-probe spectrometer equipped with a monochromatic Al-K α ray source ($h\nu = 1486.6$ eV). Data were collected at 55° takeoff angle in the hybrid mode with approximately 5 nm sampling depth, using a pass energy of 150 eV. Three spots for each sample were analyzed. The reported data were averaged over multiple spots. Analysis was performed on the Service Physics ESCA2000 A analysis software (Bend, OR). To facilitate analysis, an aminated, fluorine-tagged molecule (hexafluorobenzamide) at a concentration of 2.5 mM in 0.1 M pH 10 sodium carbonate buffer was used to mimic the reaction of an amino-bearing sugar with the DVS+ membrane.

Chemistries to modified cellulose might also alter the cellulose in ways that would detract from its material advantages (e.g., low cost, lateral flow, stability). To investigate the possibility of a deleterious morphological change to cellulose as a result of the DVS activation step, the membranes' surfaces were prepared for scanning electron microscopy (SEM). Samples of the DVS+ and DVS- membranes were coated with 5 nm of a gold-palladium alloy with an SPI

Module™ sputter coater. SEM micrographs of the membranes were acquired with an FEI Sirion SEM at the University of Washington Nanotechnology User Facility, using a spot size of 3 and a 10 kV beam accelerating voltage.

Tensile Strength Characterization of Modified and Unmodified Cellulose.

There was also concern regarding changes to the integrity of the modified cellulose, which would alter handling considerations for use in research or clinical purposes. To investigate the possibility of such changes, untreated and DVS+ membranes were tested for their tensile strength using a Thwing Albert Model EJA II Universal Testing Machine at the University of Washington Paper Science and Engineering Laboratory. 12.0 cm x 3.0 cm sheets of the membranes were affixed onto the two grips of the machine and pulled until the sample experienced necking, which refers to the deformation of the cross-sectional area in the cellulose sheet. The maximum of the stress-strain curve (achieved at the necking point) was defined as the tensile strength.

Lateral Flow Characterization of Modified and Unmodified Cellulose and Nitrocellulose

While morphological investigation may hint at any possible changes to the capillarity of the activated paper, actual LF characteristics are also important to document for future users. To determine the lateral flow speeds of various membranes, 1.0 cm x 7.0 cm strips of DVS-, DVS+, fresh chromatography paper, and nitrocellulose were cut and marked longitudinally in 1 cm increments up to 4 cm. Green food dye-colored water was poured to a depth of 0.1 cm in a 100 mL graduated cylinder. Strips of each type of membrane were dipped into the water, and the time

at which the water front in the strip reached each centimeter mark up to 4 cm was recorded.

These tests were run in triplicate for each type of membrane.

Preparation of Labeled Carbohydrate-Binding Protein Probes

Horseradish peroxidase (HRP)-labeled and Dylight 649-labeled carbohydrate-binding proteins (lectins) were employed to detect unmodified and modified carbohydrates and glycoproteins on the functionalized membrane. Con A-HRP in HEPES-T (0.05% TWEEN® 20 w/v in HEPES) interacts with immobilized mannose, maltose, glucose, aminated mannose, and RNase B.30 RCA120-HRP in PBS-T interacts with immobilized galactose, lactose, and aminopropyl galactose. 31 For fluorescent detection, Con A and RCA120 lectins were labeled with Dylight 649 amine-reactive dye. Dylight 649 containing an N-hydroxysuccinimide (NHS) ester was added to the lectins in the appropriate buffer (e.g., Con A in HEPES), incubated in an orbital shaker for 1 h at room temperature, and dialyzed for 16 h against the appropriate buffer (e.g., Dylight 649-labeled Con A against HEPES) to remove unreacted dye.

Preparation of Labeled Nucleotide Probes.

Dylight 649-labeled oligonucleotide sequences (A and A') in hybridization buffer (0.3 M NaCl, 20 mM phosphate, 2 mM EDTA, 0.6 M sodium dodecyl sulfate) were employed to detect immobilized sequences (refer to Appendix 1 for additional detail on the use of the nucleotide probes). Both sequences were labeled with Dylight 649 fluor on their 5' ends, as described for labeling the carbohydrate-binding proteins.

Colorimetric Detection of Immobilized Biomolecules

Colorimetric assays of the activated and functionalized cellulose membranes were operated on the Bio-Dot apparatus (Bio-Rad laboratories, Hercules, CA). Reagents were added successively to the sheets; each reagent was vacuumed through at 5.0 in Hg pressure before addition of the next reagent. See Figure 3 for more detail on the Bio-Dot setup.

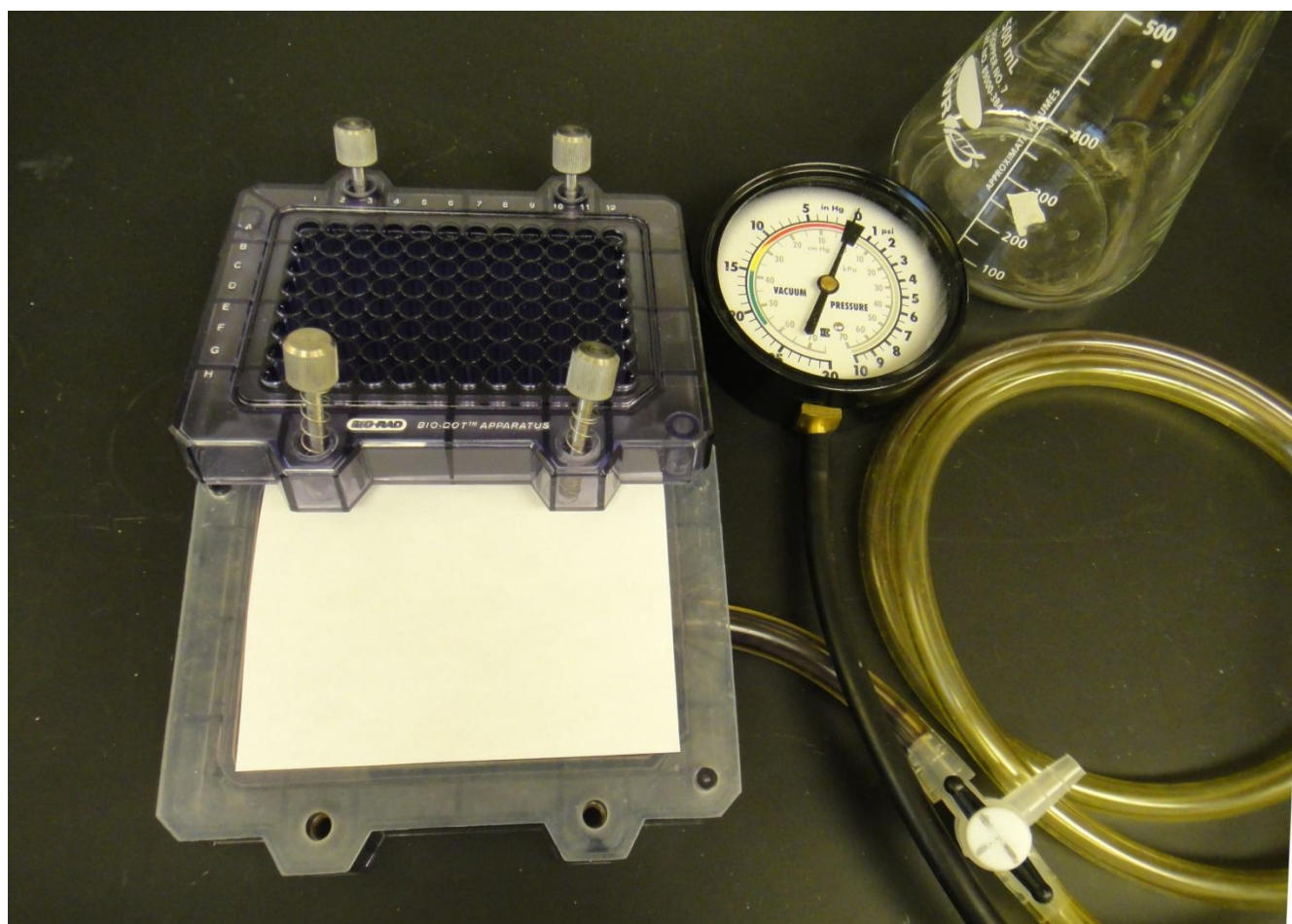


Figure 3. Bio-Dot apparatus with 96-well sample template that secures to the vacuum manifold via screws, a cellulose membrane for assaying, rubber sealing gasket sandwiched between the template and vacuum manifold, and vacuum tube extending out from the manifold. Here the tube connects to an intermediate waste container in which the assay waste solutions from the Bio-Dot are deposited.

100 μL /well of PBS was first added to rehydrate the sheet. 200 μL /well of HRP-labeled probe solution was added and vacuumed through, and the membrane was incubated for 10 minutes to allow the probes to bind to the immobilized biomolecules. Following incubation, 1200 μL /well of washing buffer (0.05% w/v TWEEN® 20, 0.1% w/v BSA in PBS) was vacuumed through to rinse unbound probes and block the surface. 100 μL /well of tetramethylbenzidine (TMB, Gaithersburg, MD) was added and vacuumed through to obtain a colorimetric readout (the reaction between HRP and TMB produces a blue colored substrate which is apparent on the paper); the color developed in approximately one minute. The sheet was then scanned on a Canon LiDE 600F desktop scanner (Canon Inc., Lake Success, NY).

Fluorometric Detection of Immobilized Biomolecules

To demonstrate the flexibility of the membranes to various detection regimes, fluorometric assays of the activated and functionalized cellulose membranes were operated on the Bio-Dot apparatus. Reagents were added successively to the sheets; each reagent was vacuumed through at 5.0 in Hg pressure before addition of the next reagent. 100 μL /well of PBS was first added to rehydrate the sheet. 200 μL /well of Dylight 649-labeled probe solution was added and vacuumed through, and the membrane was incubated for 10 minutes to allow the probes to bind to the immobilized biomolecules. Then 1200 μL /well of washing buffer (0.05% w/v TWEEN® 20, 0.1% w/v BSA in PBS) was vacuumed through to wash off unbound probes and block the surface. The sheet was scanned on a Storm 865 system (GE Healthcare Bio-Sciences Corp., Piscataway, NJ) to obtain a fluorometric readout.

Analysis of Assayed Membrane

Scanned images obtained from either the Canon desktop scanner or Storm 865 scanner were analyzed with image analysis software to measure the bioactivity of the functionalized membranes. Colorimetric assay results were scanned as .tiff images at 600 dpi. The images were imported into ImageJ software, converted to grayscale, and inverted. Because the 96-well format of the Bio-Dot apparatus imprinted the shape of the 0.45 cm-diameter circular well walls into the intensity profile of each spot after assay operation, the region of interest (ROI) was easy to identify as an outlined circle on the grayscale and inverted image. Each ROI is exactly the same area in size; as the ROI Manager in ImageJ allows the duplication of a selected ROI, only the first ROI was manually selected. All of the ROIs in the ROI manager were analyzed at the same time for Integrated Density (ID) and that data was exported to Microsoft Excel. The analysis process in ImageJ is depicted in Figure 4.

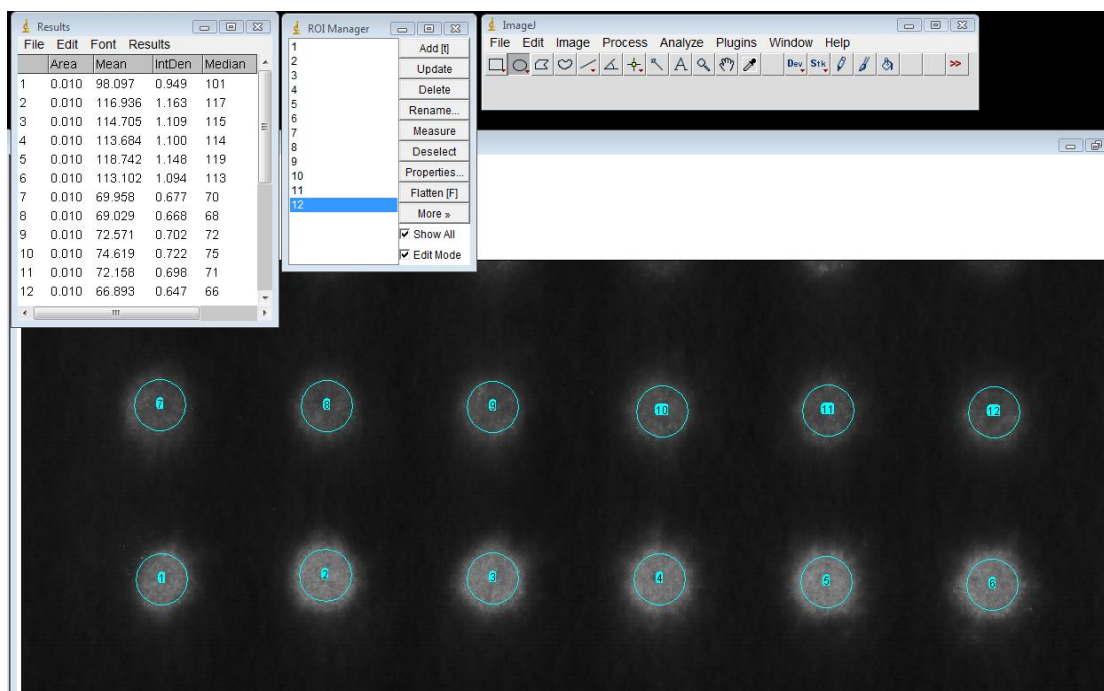


Figure 4. Desktop capture of the ImageJ interface used for ROI analysis of a colorimetric assay result. Twelve ROIs are selected via duplication of the first ROI selected using the ROI Manager. All of the ROIs can then be analyzed, and the Integrated Density (“IntDen”) is reported in the Results window for each ROI.

Scanned fluorometric intensities were analyzed with ImageQuant TL (GE Healthcare) with circular ROIs for fluorescent intensity. ROI selection was conducted in the same fashion as it was done in ImageJ, as the fluorescent assays on the Bio-Dot produced similarly imprinted well shapes onto the intensity profile. The resultant fluorescent intensities were exported to Microsoft Excel.

Mean IDs, fluorescent intensities, and standard deviations for spots immobilized with the same biomolecule were calculated in Microsoft Excel. When appropriate, Student's t-tests were employed at $p = 0.05$ to determine whether intensities of biomolecule spots on the membranes were statistically higher than the control row, and whether intensities on the DVS+ membrane were higher than the corresponding spots on DVS- membranes. Limit of detection (LOD) was determined via a Student's t-test ($p = 0.05$) for a significant difference in intensity between spots tested with a given concentration of probe and those tested with buffer only (absence of probe).

Results and Discussion

Cellulose Surface and Material Characterization

XPS surface analysis was performed to verify DVS-activation and functionalization. As shown in the XPS elemental composition results (Table 2), only carbon and oxygen were detected at the interface of unmodified cellulose membranes. After DVS-activation, the appearance of a sulfur signal in the XPS spectrum indicates that DVS successfully modified the cellulose substrate. A fluorine-containing aminated probe (F-tag depicted in Appendix 1) was used to mimic the reaction of amino-bearing biomolecules with DVS+ cellulose. After application of the F-tag, fluorine could be observed by XPS on the DVS-activated (DVS+) membrane. Based on the quotient of the observed F/S ratio by the theoretical maximum F/S ratio (each DVS bound to cellulose binds with one F-tag), 19% of the DVS molecules were observed to have reacted with the F-tag. On the unmodified membrane that was treated only with the buffer (DVS-) and spotted with F-tag, no fluorine was detected, which demonstrates the dependence on DVS for immobilization to the cellulose substrate. This data validated the ability of the DVS conjugation strategy to covalently immobilize amine-bearing molecules on DVS-activated paper.

Table 2. Relative Compositions of Functionalized Cellulose Determined by XPS

| | Cellulose | Cellulose + DVS | Cellulose + DVS + F-tag | Cellulose + F-tag |
|------|------------|-----------------|-------------------------|-------------------|
| C 1s | 57.7 ± 0.2 | 58.6 ± 0.6 | 56.9 ± 0.1 | 58.0 ± 1.6 |
| O 1s | 42.3 ± 0.2 | 40.0 ± 0.8 | 40.5 ± 0.3 | 42.0 ± 1.6 |
| S 2p | n/d | 1.4 ± 0.2 | 1.2 ± 0.3 | n/d |
| F 1s | n/d | n/d | 1.4 ± 0.2 | n/d |

Note: n/d = not detected

SEM micrographs illustrate the morphology of DVS+ cellulose compared with the DVS- control membrane. No apparent difference in morphology or fibrosity was observed between the two

samples at magnifications ranging from 32x to 500x. A comparison of the micrographs at 500x is depicted in Figure 5. These similarities suggest that DVS modification results in little to no alteration of the gross morphologic characteristics of cellulose fibers as a result of DVS cross-linking. These results suggest that DVS-modification will have minimal impact on the capillarity and LF suitability of the DVS-activated cellulose membranes. Tensile strength measurements of modified and unmodified cellulose showed a modest change in the material properties of the paper, with a decrease in tensile strength from 49 ± 3 N/m² to 34 ± 3 N/m² (DVS+). However, the modified paper demonstrated no significant difference under routine handling, printing, and assay development.

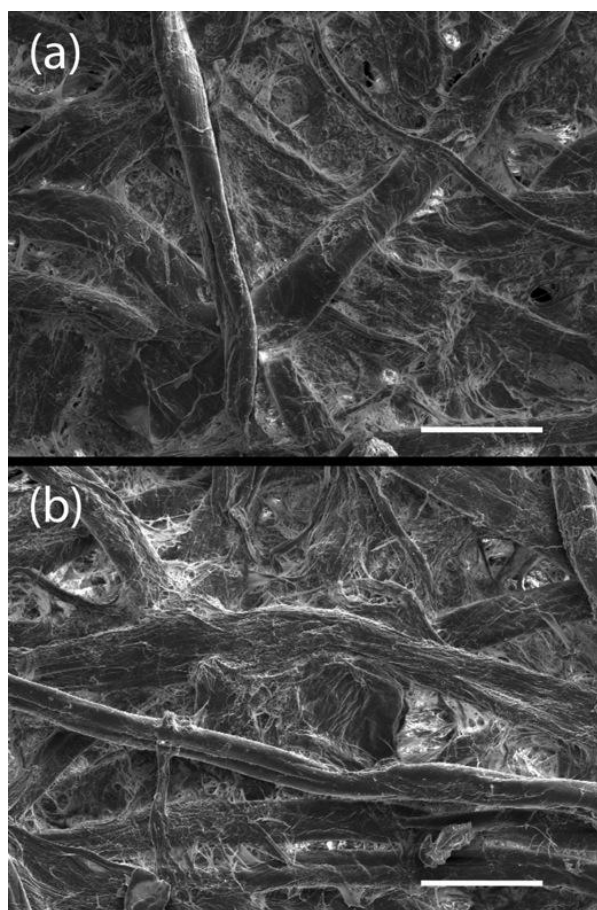


Figure 5. SEM micrographs at 500x magnification of cellulose membranes: (a) DVS- cellulose membrane (b) DVS+ cellulose membrane. Scale bar: 50 μ m (Photo credit, Lauren Cummings).

Lateral Flow Speed of Modified and Unmodified Cellulose and Nitrocellulose

Lateral flow tests for water through various types of cellulose membranes were conducted to determine the effect of DVS activation on the wicking character of cellulose. Figure 6 shows that the wicking speed of the activated (DVS- and DVS+) chromatography paper increases significantly from that of fresh chromatography paper and nitrocellulose, whose wicking speeds are evidently similar to each other. It should be noted that the time it took nitrocellulose to wick 4 centimeters was 140 seconds, which is reasonably close to the stated capillary speed of 135 seconds for 4 centimeters. The increase in the wicking speed is approximately 2/3 times, or 66%, across the various distances depicted in Figure 6. The similarity of the wicking speeds across the DVS+ and DVS- membranes suggests that the wet activation process itself, irrespective of the presence of DVS, is responsible for most of the alteration.

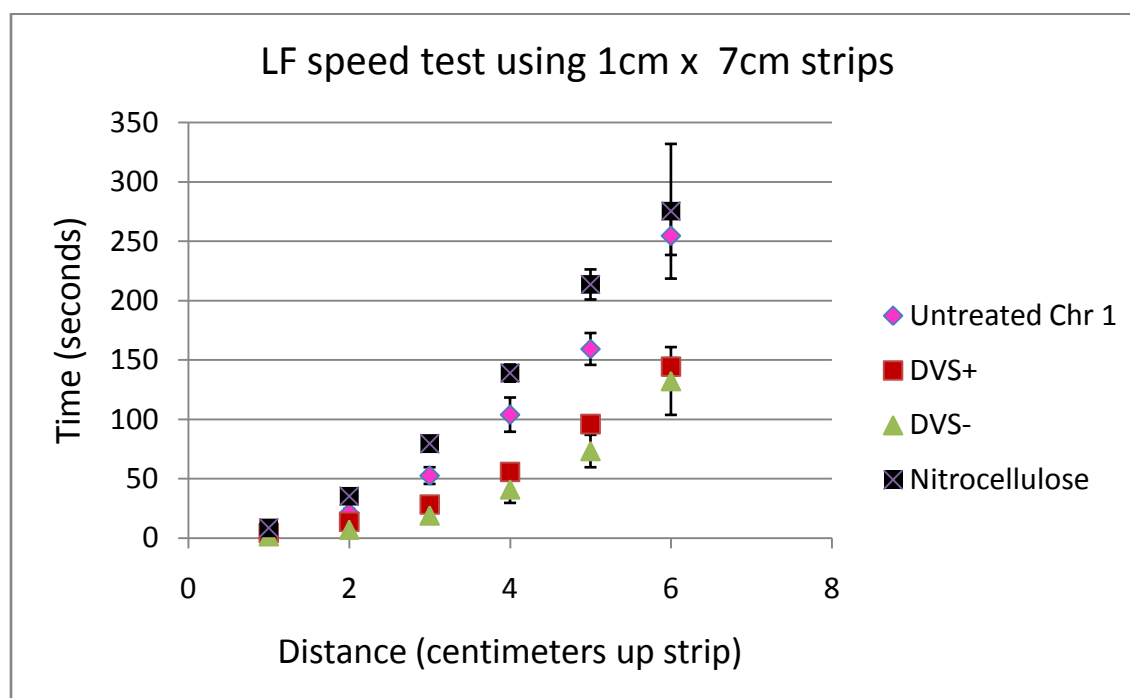


Figure 6. Wicking speed of water through fresh chromatography paper, DVS+ and DVS- and nitrocellulose strips (n=3). Nitrocellulose (along with fresh chromatography paper) achieves a speed very close to its stated capillary speed of 135 seconds/4 cm. DVS+ and DVS- membranes wick significantly faster than the former membranes, and their similarity in speed suggests the change arises from the wetting process instead of an effect from DVS activation.

Detection of Carbohydrate-Protein Interactions

To examine the capabilities and versatility of DVS-activated cellulose in conjugating bioactive molecules, we immobilized unmodified, aminated oligosaccharides and glycoprotein on cellulose membranes and determined the bioactivity via colorimetric and fluorometric lectin-binding assays. The results of the colorimetric assays in Figure 7 show the binding response of two lectins to DVS-immobilized glycans vs. glycan non-specifically adsorbed on DVS- (control) paper. On the DVS+ papers, ricin (RCA120) exhibited specific binding to the carbohydrates containing a β -galactose moiety (including aminopropyl galactose, galactose, and lactose), but no response to glycans with mannose residues (including mannose and RNaseB, Figure 7a). By contrast, Con A only shows binding to Con A-specific glycans (including mannose, glucose, maltose and RNase B, Figure 7b). The control rows on DVS+ membranes show little to no binding of either lectin, which demonstrate that non-specific binding is negligible. On the control membrane (DVS-) both lectins show minimal non-specific binding to physisorbed glycans. These results suggest that the carbohydrate-protein interactions documented on the DVS+ membranes are specific.

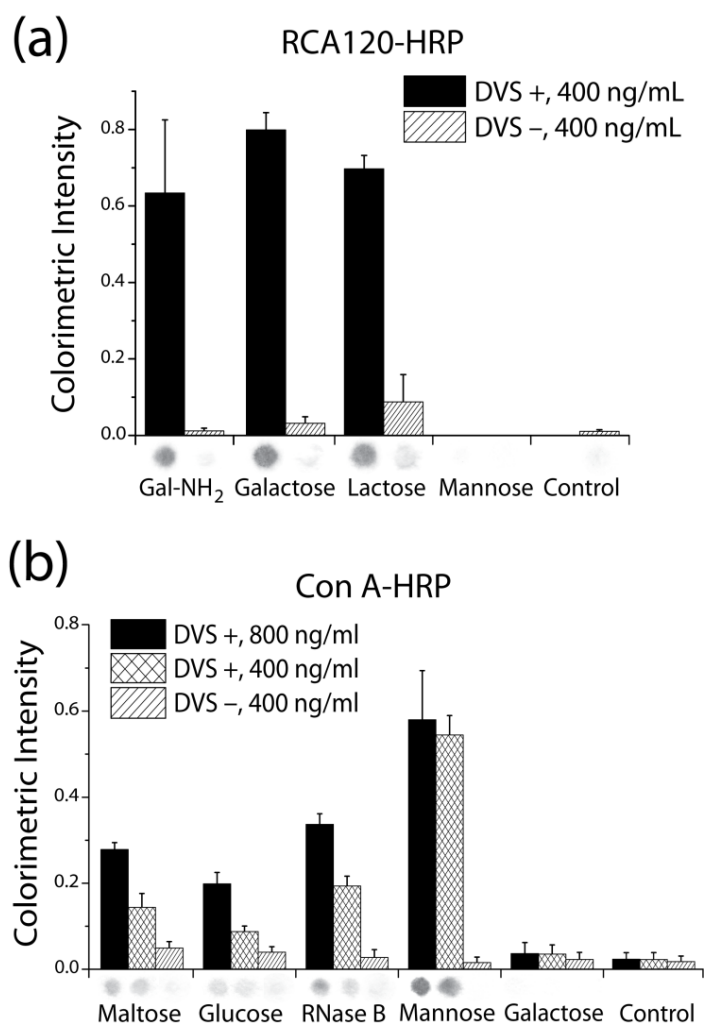


Figure 7. (a) Galactose, lactose, and aminopropyl galactose (gal-NH₂) were probed with 400 ng/mL RCA120-HRP; glycan bioactivity was observed on the DVS+ membrane but not on the DVS- membrane. There was no signal from the mannose and control (no glycan functionalized) spots, indicating that non-specific binding of RCA120 was negligible. (b) Maltose, glucose, RNase B, and mannose were bound by Con A-HRP on the DVS+ membrane but not the DVS- membrane. There was little signal from the galactose and control spots, indicating that non-specific binding of Con A was negligible. Representative colorimetric spots from the membranes appear below each corresponding bar (data were averaged over 6 spots for each carbohydrate).

Dose-dependent responses from the galactose-RCA120 and mannose-Con A interactions were observed when varying the concentration of both lectins. For RCA120-HRP, response saturated at approximately 500 ng/mL (4.8 nM), with the response of the lowest concentration tested (100 ng/mL, or 0.96 nM) well above background (Figure 8). For Con A-HRP, response saturated at

approximately 1000 ng/mL (9.6 nM), while the limit of detection (LOD) was determined to be 10 ng/mL (96 pM).

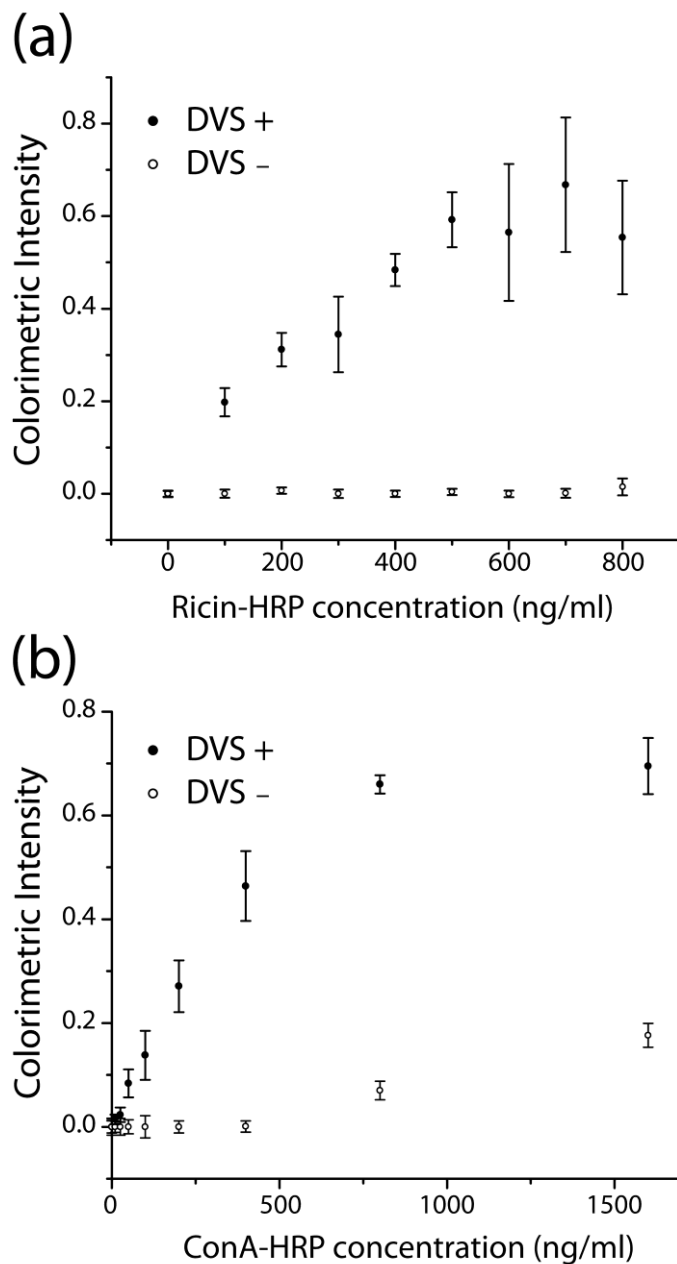


Figure 8. (a) Dose-dependent response of the RCA120-hrp-galactose interaction on DVS-activated cellulose functionalized with 555 mM galactose, for increasing RCA120-hrp concentrations. Response saturated at approximately 500 ng/mL, (4.8 nM), while the lowest signal was approximately 0.96 nM. (b) Dose-dependent response of the Con A-hrp-mannose interaction saturated at approximately 1000 ng/mL (96 nM), while the limit of detection was determined to be 10 ng (96 pM).

The fluorometric assays for immobilized carbohydrates and glycoprotein demonstrated the same specific binding observed in the colorimetric analysis. Figure 9 depicts specific binding of aminopropyl mannoside, mannose and galactose (negative control) by Dylight 649-labeled Con A. As previously observed, amino-modified glycans show significantly higher conjugation efficiency, as indicated by their increased bioactivity at a given immobilization concentration.²⁷

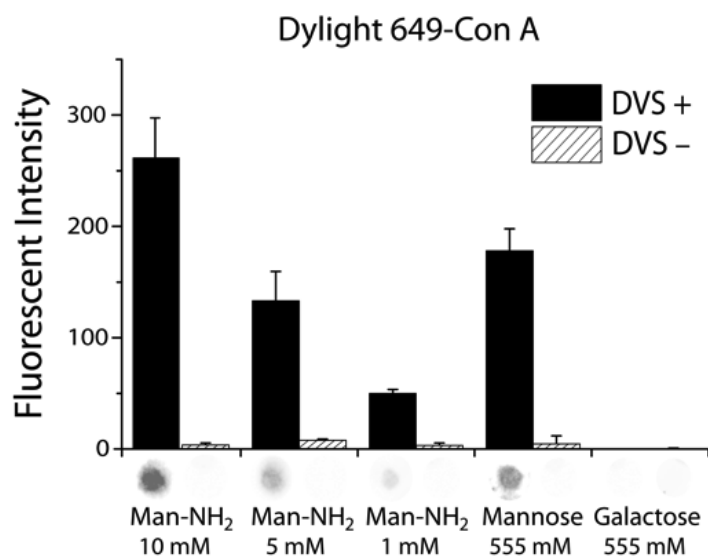


Figure 9. Aminopropyl mannoside (man-NH₂) and mannose were probed with 50 nM Dylight 649-labeled Con A; bioactivity was observed on the DVS+ membrane but not on the DVS- membrane. There was no signal from the galactose spots, as expected. Representative fluorometric spots from the membranes appear below each corresponding bar (data were averaged over 6 spots for each carbohydrate).

Both the colorimetric and fluorometric assays demonstrate that DVS-modified cellulose paper is suitable for conjugation of carbohydrates and analysis of biological interactions using various means of detection. Aminated and hydroxylated biomolecules were successfully conjugated onto the paper with apparent efficiencies reflecting their nucleophilicity. These interactions have been demonstrated to be semi-quantitative, as variations in the concentration of immobilized biomolecules and the probing lectins yield statistically and visually significant differences in response.

It is worth noting that the DVS chemistry enables direct conjugation of free oligosaccharides onto cellulose through a vinylsulfone-hydroxyl reaction, dramatically reducing the burden of chemical modification of carbohydrates. While the selectivity of this reaction could be complicated by the multiple hydroxyls presented by a carbohydrate molecule, we previously conducted work demonstrating that the majority of free sugars are linked via the anomeric hydroxyl.²⁷ To investigate the vinyl sulfone reaction preference for hydroxyl groups in saccharides we studied a model reaction of ethyl vinyl sulfone (EVS) and free mannose in solution. Using thin-layer chromatography and Nuclear Magnetic Resonance spectroscopy we found that ~90 percentage of EVS-mannose products react at anomeric position, and the ratio of α - and β - isomers is around 3:1, which is close to the ratio of free mannose in solution.²⁷

Detection of FITC-Alginate

Alginate, a polysaccharide harvested from brown algae, has been proposed for use in valves on microfluidic cellulose networks by the Yager research group at the Department of Bioengineering. In Gina Fridley's preliminary work, incubated clumps of alginate precluded water flow through branches of nitrocellulose when calcium ions were previously applied. On the other hand, subsequent application of sodium ions were able to disperse the calcium alginate complex and allow flow through the branch. However, the weak binding of physically-adsorbed alginate on nitrocellulose resulted in the alginate being dispersed out of the intended valve areas on the nitrocellulose networks. DVS chemistry may be able to immobilize alginate more strongly and contribute towards more durable alginate-mediated valves on cellulosic networks. To this end, an experiment to immobilize FITC-labeled alginate onto DVS+ membranes was conducted. Figure 10 demonstrates that FITC-labeled alginate remains on the DVS+ membrane after

washing off all of the loosely-bound alginate. This demonstrated that DVS has some potential for the immobilization of alginate to create more robust valves. Furthermore, this experiment featured two different types of chromatography paper, 1 Chr and 20 Chr, which feature larger and smaller pore sizes, respectively. The higher fluorescent response on the 20 Chr DVS+ membranes suggests that a smaller pore size and higher density of cellulose fibers yields a higher amount of immobilized ligands per unit area.

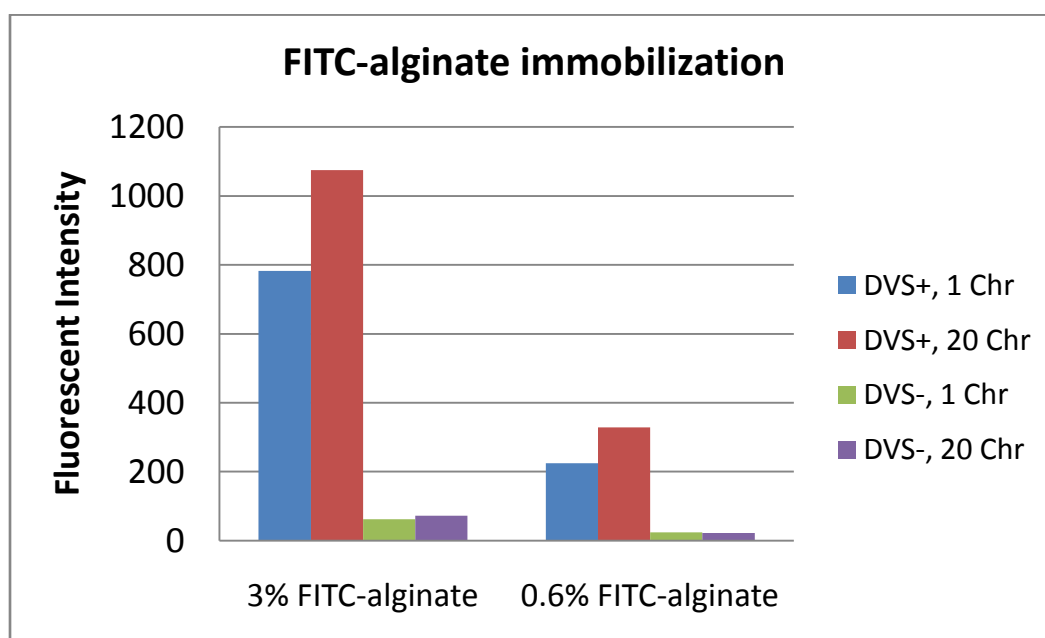


Figure 10: Fluorescent response of 3% and 0.6% w/v FITC-labeled alginate on DVS+ and DVS- membranes. Bioactivity was observed on the DVS+ membrane, with much smaller response on the DVS- membrane.

Detection of DNA Oligonucleotide Hybridization

Nucleic acid tests (NATs) are valued in clinical diagnostics for their ability to sense pathogens, by detecting the genetic material of viruses, bacteria and protozoa. The development of NATs in a lab-on-a-chip or paper-based format for low-resource settings has received considerable attention.^{2,6,21, 32} To demonstrate the suitability of DVS-modified cellulose for DNA detection, we performed a simple hybridization assay (See Appendix 1). We observed binding of a labeled

sequence (A') to spotted rows of the immobilized sequence (A) but not to the control row on DVS+ membranes (Figure 11a), indicating that DNA hybridization can be detected on the DVS-activated cellulose and non-specific binding of sequence A' to the surface was negligible. A labeled non-complementary sequence (A) was incubated as a negative control on both the DVS+ and DVS- membranes, with no observed binding to the immobilized sequence (A) on either membrane. These results suggest that the incubated sequence A' was specifically hybridized to immobilized sequence A on the DVS+ membrane. In a separate experiment, a dose-dependent response of the DNA-functionalized membrane was observed by varying the concentration of the probing sequence (A') (Figure 11b).

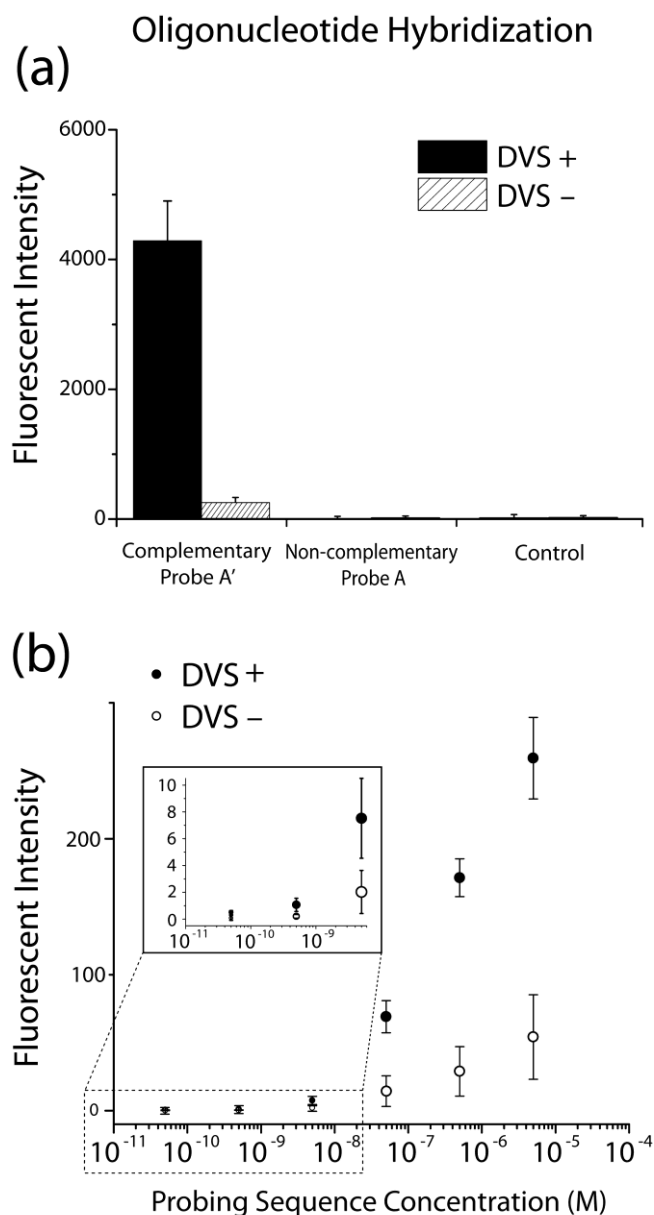


Figure 11. (a) Immobilized sequence (A) was probed by 5 μM of the complementary probe sequence (A'); bioactivity was observed on the DVS+ membrane but not the DVS- membrane. Labeled sequence (A) was also incubated as a negative control, and was not detected on either membrane. The control row (no oligonucleotides functionalized) also showed no response to incubated A', indicating that non-specific binding of the sequence was negligible. **(b)** Dose-dependent detection of immobilized sequence (A) was observed for concentrations of probe (A') from 0.5 nM to 5 μM .

We observed a significant signal difference between the DVS+ and DVS- membranes, in accordance with the role played by DVS in covalent immobilization of the oligonucleotide target. The hybridization observed on the DVS- paper can be attributed to a low-level of physisorbed target sequence (non-covalent) to the unmodified cellulose. However, DVS yielded

an order of magnitude higher response for the hybridization assay. The limit of detection (LOD) of this non-optimized system was found to be 500 pM. This result is on-par with those reported for short oligonucleotide hybridization on zirconia-modified filter paper (using FITC-labeled probe),³³ and on gold using surface plasmon resonance imaging (SPRi) (unlabeled probe).³⁴

Detection of Protein-Protein Interactions

We have also immobilized an immunoglobulin G antibody (anti-Streptavidin) and attempted to detect it using HRP-labeled streptavidin in a colorimetric assay. The bioactivity detected was very similar in magnitude on both DVS- and DVS+ membranes (Figure 12). This suggests that the physical adsorption of the antibody onto cellulose was sufficiently strong enough to avoid being broken by the washing buffer. We hypothesized that the presumably covalently-immobilized antibody on the DVS+ membranes may be more stable over time than the physically adsorbed antibody on the DVS- membranes, and duplicated our experiments one week and one month after the functionalization time. Figure 12 also shows that these experiments demonstrate that DVS reactivity does not help with stabilizing the antibody on the surface. In fact, it seems that the signal from the antibody-streptavidin interaction on the DVS+ membrane is actually weaker. We now hypothesize that the DVS-based modification interferes with the electrostatic interactions that may otherwise strengthen the adsorption of proteins with cationic character such as IgGs to cellulose.

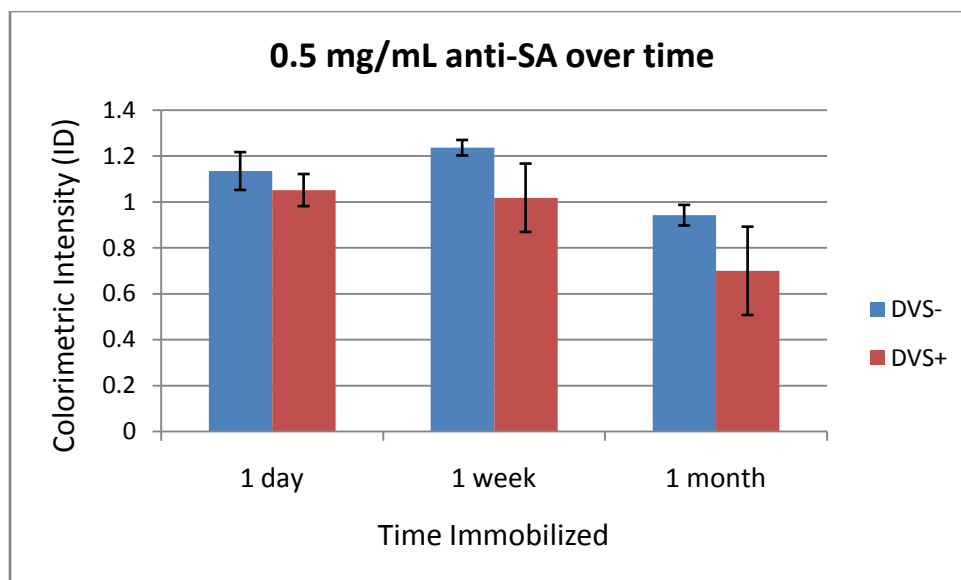


Figure 12. Immobilized antibody anti-Streptavidin was probed by HRP-labeled streptavidin. Bioactivity was observed on both DVS+ and DVS- membranes, in similar magnitudes. Two further experiments with functionalized membranes stored for 1 week and 1 month demonstrate the same general trend, with some loss in activity on the DVS+ membranes. This indicated that non-specific binding of anti-Streptavidin was strong and sufficient to yield a stable protein-functionalized membrane.

Stability of DVS-activated Cellulose

To develop a reliable paper-based platform suitable for future point-of-care applications, the stability of DVS-activated and biofunctional cellulose is critical. A cellulose-based LF platform for low-resource settings needs to maintain its stability for extended periods of time. To gain a better understanding of the stability of our DVS-cellulose platform, we tested the stability of DVS-activated membranes after 60 days of storage under two conditions. Carbohydrates and the glycoprotein RNase B were spotted on the membranes after the storage period and tested for specific binding to labeled Con A. First, an experiment involving DVS-activated membranes membrane stored for 30 days in ambient conditions (on the lab bench) suggested that there was not a significant decrease in reactivity of the DVS over time (Figure 13).

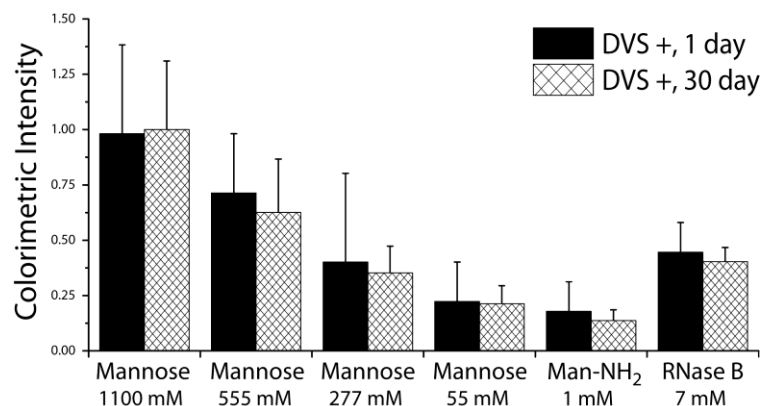


Figure 13. Colorimetric analysis of intensities of biomolecule spots on DVS-activated membranes does not reveal significant differences between membranes functionalized the day of DVS activation, and membranes functionalized 30 days after being stored in aluminum foil. A Student's t-test with $p = 0.05$ did not yield any significant differences between any of the 1 day-30 day pairs.

Subsequently, another experiment using more controlled storage conditions was conducted using a dry, nitrogen-filled box. The results in Figure 14a indicate that the activity of carbohydrates and glycoprotein spotted on the aged DVS-cellulose was very similar to that of freshly activated DVS-paper. Only minor variability was observed for the immobilized mannose. We ascribe these minor differences to physical irregularities within the manufactured chromatography paper used for this study; the inconsistencies within the Chr 1 paper are apparent on visual inspection and may affect the degree of DVS activation, biomolecule immobilization, and therefore probe response. However, this heterogeneity results in only modest standard deviations for the bioactivity of the immobilized carbohydrates, glycoprotein and oligonucleotide. These results demonstrate that DVS-activated cellulose is stable to prolonged storage while retaining reactivity for subsequent biomolecule immobilization.

Having established that DVS-activated membranes retain their reactivity after prolonged storage, we investigated the ability of biofunctional DVS+ membranes to retain their bioactivity following storage at room temperature. We tested the stability of a DVS-activated membrane functionalized with carbohydrates and glycoprotein and stored in a dry, non-sterile, nitrogen-

filled environment for 30 days. Following storage, Con A binding showed preservation of the bioactivity with differing amounts of loss, varying by specific glycans (Figure 14b). These results demonstrate that biofunctional DVS-cellulose has potential as a robust platform with an extended shelf-life for point-of-care diagnostics and other applications.

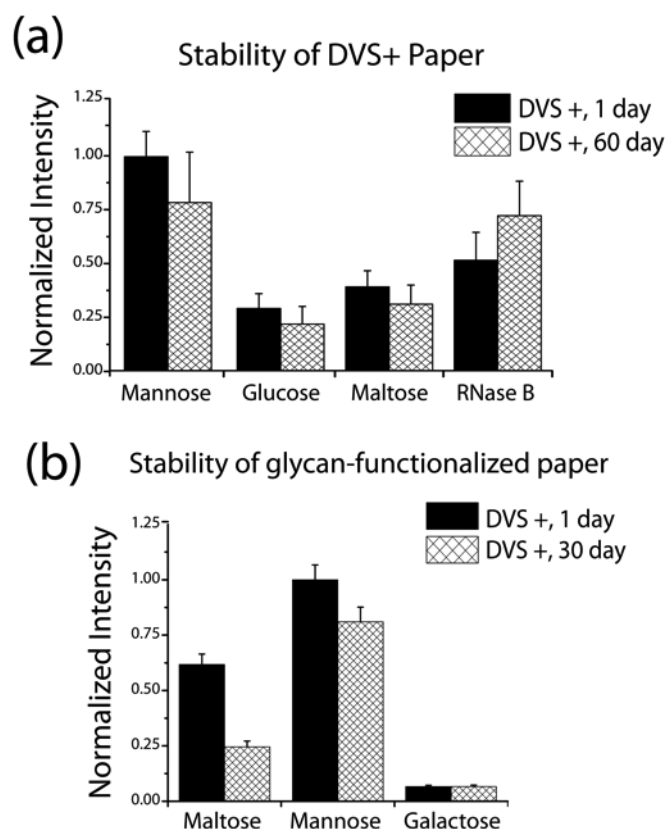


Figure 14. (a) DVS-activated membranes were stored for 60 days and subsequently functionalized with mannose, glucose, maltose, and RNase B. The bioactivity, as observed by fluorescent ConA detection, was minimally affected by storage of the DVS-activated paper. (b) Biofunctional DVS+ membranes stored for 30 days retained significant bioactivity. The aged membranes experienced slight bioactivity loss for mannose and a more significant loss for maltose, when compared to a membrane freshly functionalized and assayed. Loss in bioactivity for the maltose-functionalized membrane may be ascribed to its susceptibility to degradation by microbiota in the non-sterile storage environment.

Printed Biomolecular Patterning

Fabrication of biomolecular patterns on LF-based cellulosic diagnostic devices may benefit from the development of facile bioprinting techniques.^{35, 36} To demonstrate the adaptability of the

DVS functionalization technique to bioprinting we have visualized patterns of immobilized galactose on DVS-activated cellulose membranes using fluorescently labeled RCA120. An Epson R280 inkjet printer was modified for printing biological solutions. The printing solution we formulated (10% w/v galactose, 40% w/v sucrose and 5% w/v TWEEN® 20 in 0.1 M pH 10 sodium carbonate buffer) was previously immobilized and assayed on a DVS-activated membrane without the galactose component to ensure that the non-reducing sugar sucrose did not interfere with binding by RCA120 (not shown). Examples of the printed patterns are reproduced below in Figure 15.



Figure 15: Fluorescent patterns of the University of Washington "W" and "Husky" logos obtained by interactions of Dylight 649-RCA120 with immobilized galactose. Scale bar: 1 cm.

These visualizations indicate that DVS-activated cellulose is amenable to accurate, sub-millimeter patterning of biomolecules through bioprinting, and that the printed biomolecules retain their bioactivity following the printing process. The simplicity of this technique may facilitate the fabrication of LF-based cellulosic diagnostic devices as the printing strategy is amenable to simultaneous patterning of multiple reagents in large-scale production. Separation of the physical printing and digitized design processes also permits the rapid implementation of design changes during fabrication. In particular, production of multiplexed paper devices could be greatly expedited by the accuracy and automation presented by bioprinting.

Conclusions

We have presented a simple covalent immobilization method for cellulose using DVS chemistry. DVS-activated cellulose membranes exhibit a versatile capacity for conjugation of biomolecules presenting nucleophilic functional groups. Immobilized carbohydrates and oligonucleotides on DVS-activated cellulose membranes demonstrate specific response to lectins and complementary nucleotides, respectively. This membrane exhibits trivial amounts of non-specific binding of the aforementioned biomolecular analytes. Probing of the functionalized surface with either lectins or oligonucleotides is dose-dependent, and the LOD of nucleic acid hybridization is comparable to results observed previously using SPR and zirconia-modified paper. In addition, DVS-activated and biofunctional cellulose membranes maintain their activity for prolonged storage under ambient conditions, which demonstrates the suitability of this technique for the fabrication of paper-based bioassays for low-cost and portable point-of-care diagnostics. Finally, the DVS strategy has potential for application to broader efforts. It can be combined with inkjet bioprinting to accurately produce biomolecular patterns, demonstrating the potential of cellulose for sophisticated bioassay design and multiplexed detection. Immobilization of alginate demonstrates that DVS may also be used to increase the durability of alginate-mediated valves on cellulosic networks. These findings demonstrate that cellulose can be chemically activated with DVS for the generation of biofunctional paper with potential applications in LF-based diagnostic devices for use in molecular detection in research, diagnostics, environmental monitoring, and limited-resource molecular sensing.

References

1. von Lode, P. Point-of-Care Immunotesting: Approaching the Analytical Performance of Central Laboratory Methods. *Clin. Biochem.* **2005**, *38*, 591-606.
2. Yager, P.; Edwards, T.; Fu, E.; Helton, K.; Nelson, K.; Tam, M.R.; Weigl, B.H. Microfluidic diagnostic technologies for global public health. *Nature* **2006**, *442*, 412-418.
3. Yager, P.; Domingo, G.J.; Gerdes, J. *Annu. Rev. Biomed. Eng.* Point-of-Care diagnostics for Global Health. **2008**, *10*, 107-144.
4. Tonkinson, J.L.; Stillman, B.A. Nitrocellulose: A Tried and True Polymer Finds Utility as a Post-Genomic Substrate. *Front. Biosci.* **2002**, *7*, C1-C12.
5. Martinez, A.W.; Phillips, S.T.; Butte, M.J.; Whitesides, G.M. Patterned Paper as a Platform for Inexpensive, Low-Volume, Portable Bioassays. *Angew. Chem. Int. Edit.* **2007**, *46*, 1318-1320.
6. Pelton, R. Bioactive Paper Provides a Low-Cost Platform for Diagnostics. *Trac-Trend Anal. Chem.* **2009**, *28*, 925-942.
7. Martinez, A.W.; Phillips, S.T.; Whitesides, G.M. Three-Dimensional Microfluidic Devices Fabricated in Layered Paper and Tape. *Proc. Natl. Acad. Sci. U. S. A.* **2008**, *105*, 19606-19611.
8. Martinez, A.W.; Phillips, S.T.; Whitesides, G.M.; Carrilho, E. Diagnostics for the Developing World: Microfluidic Paper-Based Analytical Devices. *Anal. Chem.* **2010**, *82*, 3-10.

9. Fenton, E.M.; Mascarenas, M.R.; Lopez, G.P.; Sibbett, S.S. Multiplex Lateral-Flow Test Strips Fabricated by Two-Dimensional Shaping. *Acs Appl. Mater. Inter.* **2009**, *1*, 124-129.
10. Li, X.; Tian, J.F.; Shen, W. Thread As a Versatile Material for Low-Cost Microfluidic Diagnostics. *Acs Appl. Mater. Inter.* **2010**, *2*, 1-6.
11. Reches, M.; Mirica, K.A.; Dasgupta, R.; Dickey, M.D.; Butte, M.J.; Whitesides, G.M. Thread as a Matrix for Biomedical Assays. *Acs Appl. Mater. Inter.* **2010**, *2*, 1722-1728.
12. Towbin, H.; Staehelin, T.; Gordon, J. Electrophoretic Transfer of Proteins from Polyacrylamide Gels to Nitrocellulose Sheets - Procedure and Some Applications. *Proc. Natl. Acad. Sci. U. S. A.* **1979**, *76*, 4350-4354.
13. Bode, L.; Beutin, L.; Kohler, H. Nitrocellulose-Enzyme-Linked Immunosorbent-Assay (NC-ELISA) - A Sensitive Technique for the Rapid Visual Detection of Both Viral-Antigens and Antibodies. *J. Virol. Methods* **1984**, *8*, 111-121.
14. Tovey, E.R.; Baldo, B.A. Protein-Binding to Nitrocellulose, Nylon and PVDF Membranes in Immunoassays and Electroblothing. *J. Biochem. Bioph. Methods* **1989**, *19*, 169-183.
15. Jones, K.L.; O'Melia, C.R. Protein and Humic Acid Adsorption onto Hydrophilic Membrane Surfaces: Effects of pH and Ionic Strength. *J. Membrane Sci.* **2000**, *165*, 31-46.
16. Stollner, D.; Scheller, F.W.; Warsinke, A. Activation of Cellulose Membranes with 1,1'-carbonyldiimidazole or 1-cyano-4-dimethylaminopyridinium tetrafluoroborate as a Basis for the Development of Immunosensors. *Anal. Biochem.* **2002**, *304*, 157-165.

17. Bora, U.; Sharma, P.; Kannan, K.; Nahar, P. Photoreactive Cellulose Membrane - A Novel Matrix for Covalent Immobilization of Biomolecules. *J. Biotechnol.* **2006**, *126*, 220-229.
18. Sharma, P.; Basir, S.F.; Nahar, P. Photoimmobilization of unmodified carbohydrates on activated surface. *J. Colloid Interface Sci.* **2010**, *342*, 202-204.
19. Bryjak, J.; Liesiene, J.; Stefuca, V. Man-Tailored Cellulose-Based Carriers for Invertase Immobilization. *Cellulose* **2008**, *15*, 631-640.
20. Kong, D.L.; Schuett, W.; Dai, J.; Kunkel, S.; Holtz, M.; Yamada, R.; Yu, Y.T.; Klinkmann, H. Development of Cellulose-DNA Immunoabsorbent. *Artif. Organs* **2002**, *26*, 200-208.
21. Su, S.X.; Nutiu, R.; Filipe, C.D.M.; Li, Y.F.; Pelton, R. Adsorption and Covalent Coupling of ATP-Binding DNA Aptamers onto Cellulose. *Langmuir* **2007**, *23*, 1300-1302.
22. Araujo, A.C.; Song, Y.; Lundeberg, J.; Stahl, P.L.; Brumer, H. Activated Paper Surfaces for the Rapid Hybridization of DNA through Capillary Transport. *Anal. Chem.* **2012**, in press.
23. Xu, C.; Spadiut, O.; Araujo, A.C.; Nakhai, A.; Brumer, H.; Chemo-enzymatic Assembly of Clickable Cellulose Surfaces via Multivalent Polysaccharides. *ChemSusChem*. **2012**, *5*, 661-665.
24. Sereikaite, J.; Bassus, D.; Bobnis, R.; Dienys, G.; Bumeliene, Z.; Bumelis, V.A. Divinyl Sulfone as a Crosslinking Reagent for Oligomeric Proteins. *uss. J. Bioorg. Chem.* **2003**, *29*, 227-230.
25. Porath, J.; Laas, T.; Janson, J.C. Agar Derivatives for Chromatography, Electrophoresis, and Gel-Bound Enzymes. III. Rigid Agarose Gels Cross-Linked with Divinyl Sulfone (DVS). *J. Chromatogr.* **1975**, *103*, 49-62.

26. Fornstedt, N.; Porath, J. Characterization Studies on a New Lectin Found in Seeds of *Vicia-Ervilia*. *FEBS Lett.* **1975**, *57*, 187-191.
27. Cheng, F.; Shang, J.; Ratner, D.M. A Versatile Method for Functionalizing Surfaces with Bioactive Glycans. *Bioconjugate Chem.* **2011**, *22*, 50-57.
28. Shang, J.; Cheng, F.; Dubey, M.; Kaplan, J.M.; Rawal, M.; Jiang, X.; Newburg, D.S.; Sullivan, P.A.; Andrade, R.B.; Ratner, D.M. An organophosphonate strategy for functionalizing silicon photonic biosensors. *Langmuir* **2012**, *28*, 3338-3344.
29. Hayes, W.; Osborn, H.M.I.; Osborne, S.D.; Rastall, R.A.; Romagnoli, B. One-Pot Synthesis of Multivalent Arrays of Mannose Mono-and Disaccharides. *Tetrahedron* **2003**, *59*, 7983-7996.
30. Goldstein, I.J.; Hollerman, C.E.; Smith, E.E. Protein-Carbohydrate Interaction .2. Inhibition Studies on Interaction of Concanavalin A with Polysaccharides. *Biochemistry* **1965**, *4*, 876-&.
31. Olsnes, S.; Pihl, A. Different Biological Properties of 2 Constituent Peptide Chains of Ricin, a Toxic Protein Inhibiting Protein-Synthesis. *Biochemistry (Mosc)*. **1973**, *12*, 3121-3126.
32. Lutz, S.; Weber, P.; Focke, M.; Faltin, B.; Hoffmann, J.; Muller, C.; Mark, D.; Roth, G.; Munday, P.; Armes, N.; Piepenburg, O.; Zengerle, R.; von Stetten, F. Microfluidic Lab-On-a-Foil for Nucleic Acid Analysis Based on Isothermal Recombinase Polymerase Amplification (RPA). *Lab Chip* **2010**, *10*, 887-893.
33. Xiao, W.; Huang, J.G. Immobilization of Oligonucleotides onto Zirconia-Modified Filter Paper and Specific Molecular Recognition. *Langmuir* **2011**, *27*, 12284-12288.

34. Nelson, B.P.; Grimsrud, T.E.; Liles, M.R.; Goodman, R.M.; Corn, R.M. Surface Plasmon Resonance Imaging Measurements of DNA and RNA Hybridization Adsorption onto DNA Microarrays. *Anal. Chem.* **2001**, *73*, 1-7.

35. Derby, B. Bioprinting: Inkjet Printing Proteins and Hybrid Cell-Containing Materials and Structures. *J. Mater. Chem.* **2008**, *18*, 5717-5721.

36. Khan, M.S.; Fon, D.; Li, X.; Tian, J.F.; Forsythe, J.; Garnier, G.; Shen, W. Biosurface Engineering Through Inkjet Printing. *Colloid Surface B* **2010**, *75*, 441-447.

Appendix

Appendix 1: Schematics of Biomolecules, Synthesis of Hexafluorobenzamide, and DNA

Hybridization Experiments

Immobilized Biomolecules

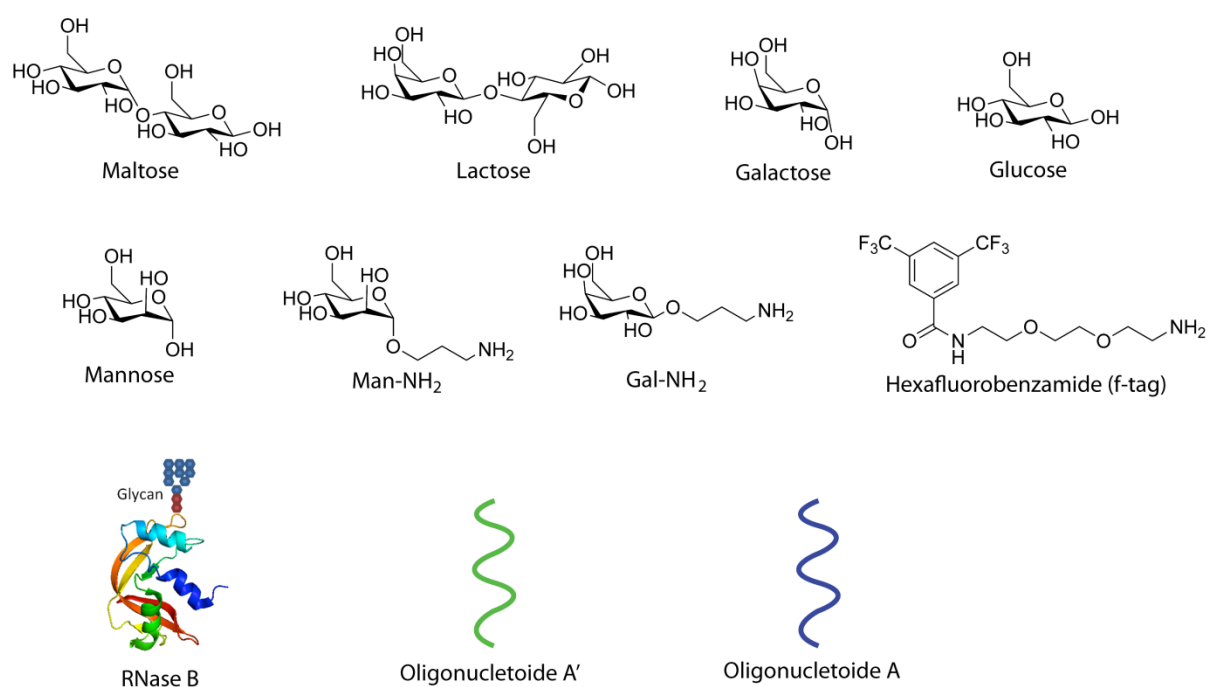


Figure 16. Biomolecules used in this work. The carbohydrates used were maltose, lactose, galactose, glucose, mannose, aminopropyl mannoside (Man-NH₂), and aminopropyl galactose (Gal-NH₂). Glycoprotein used was RNase B. Oligonucleotide sequences used were labeled A and A'.

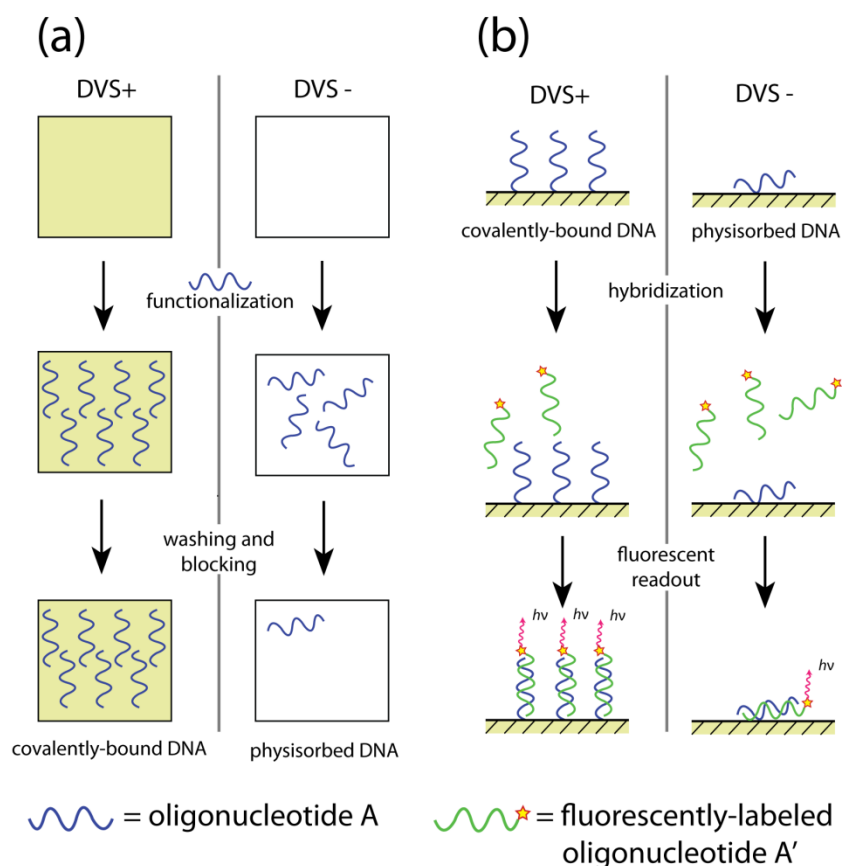


Figure 17. (a) Aminated oligonucleotide A was spotted onto DVS+ and DVS- membranes, illustrating covalent attachment to the DVS+ substrate and physisorption to the unmodified (DVS-) cellulose. Washing and blocking with PBS-T removes the majority of physisorbed oligonucleotide, while covalently-bound DNA remains on the DVS+ membrane. (b) A fluorometric DNA hybridization assay utilized Dylight 649-labeled probe sequence A' in hybridization buffer. DVS+ bound DNA on the DVS+ membranes would respond more strongly.

Appendix 2: Photographs of Bioprinter Modification

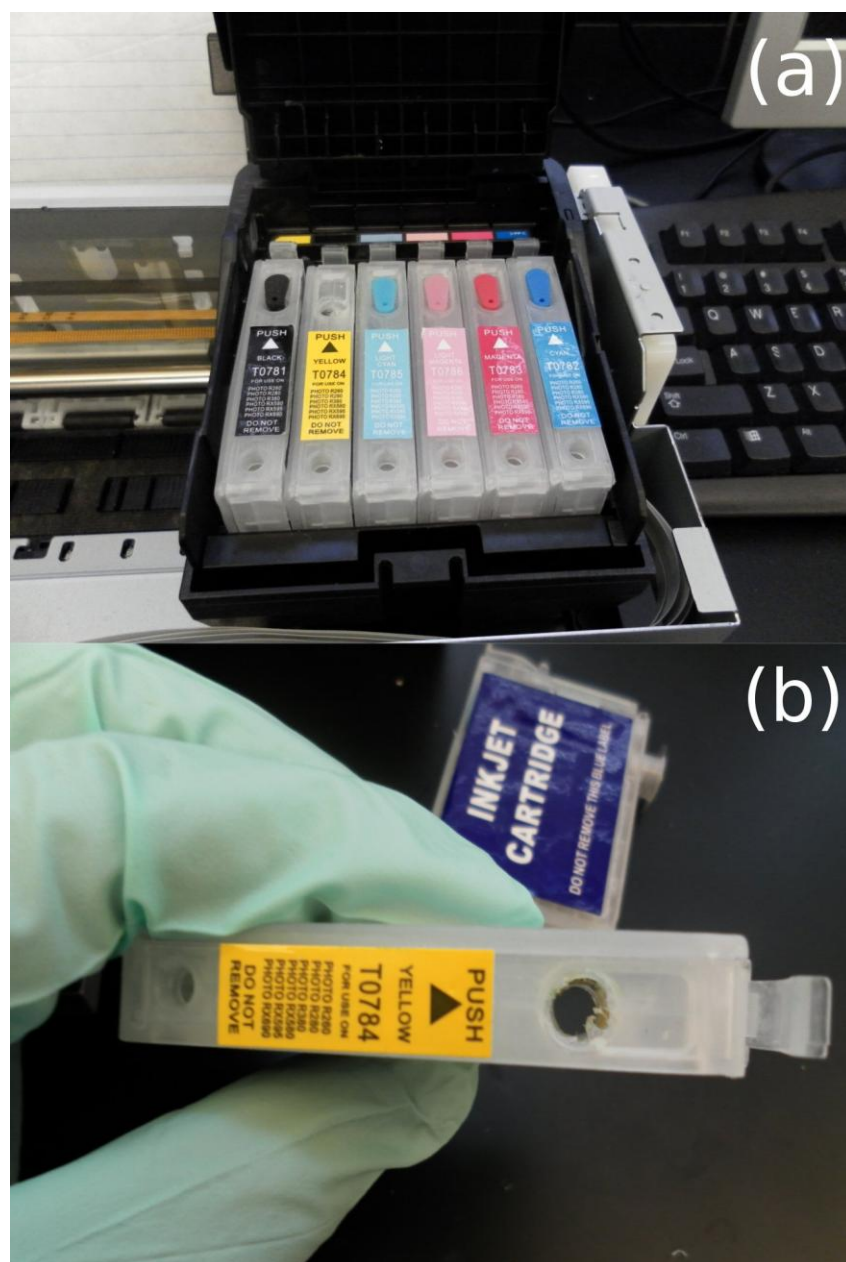


Figure 18. (a) Six empty refill cartridges replaced the original ink cartridges that shipped with the R280. This was necessary to accommodate the modifications made to one cartridge in (b). (b) Milled circular channel in the cartridge allowed room for insertion of pipette tip onto the printhead in lieu of the ink channel in the cartridge itself.



Figure 19. A pipette tip reservoir was fabricated by truncation of a 200 μL pipette tip so that the tip could be inserted onto the printhead. During printing preparation the reservoir is filled with either priming or bio-ink solution.

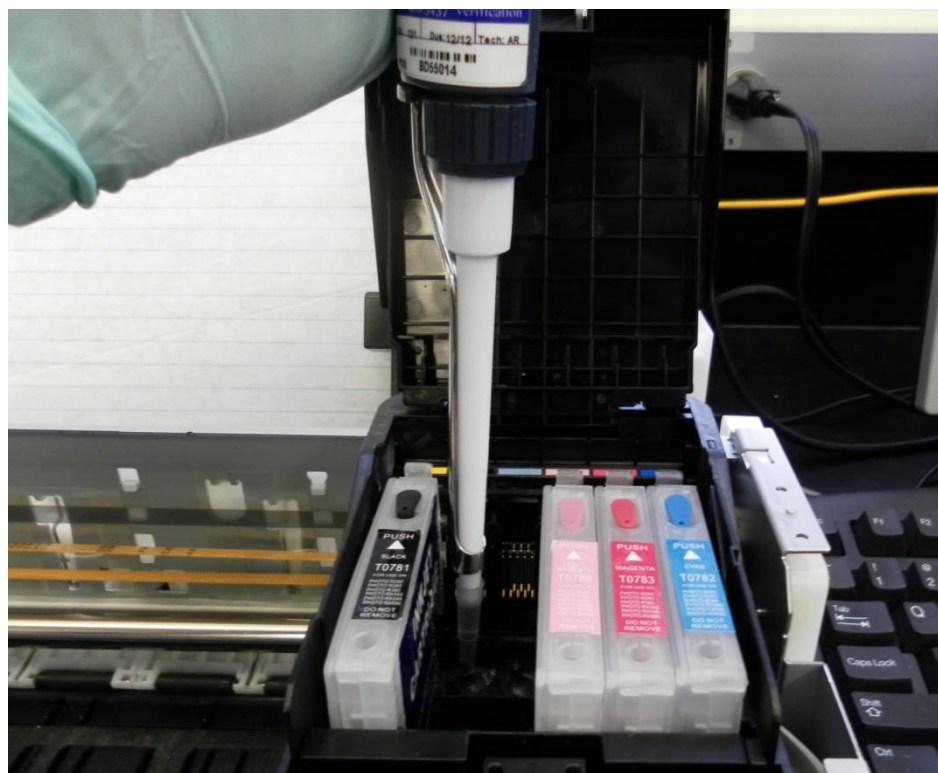


Figure 20. A pipettor was used to apply pressure and push through 50-100 μL of the bio-ink solution to fill the printhead and eliminate air bubbles which would interfere with the production of droplets in the inkjet.